Available online at www.sciencedirect.com
SCIENCE DIRECT
Quaternary International 154–155 (2006) 26–31

A lateglacial rock avalanche event, Tianchi Lake, Tien Shan, Xinjiang

Chaolu Yi[a,*], Ling Zhu[b], Yeong Bae Seong[c], Lewis A. Owen[c], Robert C. Finkel[d]

[a]Institute of Tibetan Plateau Research, Chinese Academy of Sciences, Beijing 100085, P.R. China
[b]Department of Geography, Nanjing University, Nanjing 210093, P.R. China
[c]Department of Geology, University of Cincinnati, Cincinnati, OH 45221-0013, USA
[d]Lawrence Livermore National Laboratory, Livermore, CA 94550-9234, USA

Available online 10 March 2006

Abstract

The genesis of a diamicton deposit that dams Tianchi Lake in the eastern Tien Shan, Xinjiang, China, has been debated for many years, and it has generally been considered to have been either the result of landsliding or glacial deposition. Using geomorphic, sedimentological and geochronological techniques we re-examined this deposit to help elucidate its origin. The outer margin of the deposit can be traced up the adjacent hillside, where a series of steps within the bedrock are present and likely represent landslide scars. Within the lake the deposit has an undulating surface. The deposit is unstratified, comprising angular monomictic clasts that coarsen upward into boulders, which armor the surface. All these features suggest that the deposit was formed by landsliding. Furthermore, ^{10}Be cosmogenic radionuclide surface exposure dating of boulders on the levee of the deposit show that the deposit probably formed during the Lateglacial, possibly at ~12 ka and is likely coincident to the Younger Dryas Stade. The sedimentological and geomorphic evidence support our view that the diamicton deposit is not of glacial origin, but was deposited by rock avalanching during the Lateglacial.

1. Introduction

Distinguishing the origin of mountain area landforms that comprise diamictons is difficult because of the similarities between the characteristics shown by deposits formed by mass movement and those formed by glacial action (Owen, 1991, 1993; Hewitt, 1999). Hewitt (1999) highlighted these problems in the Karakoram Himalaya when he showed that some deposits previously identified as terminal moraine complexes were actually emplaced by rock avalanches. Sedimentary properties and geomorphological features of rock avalanches were examined extensively in other areas (Owen, 1991, 1993; Bishop, 1997; Friedmann, 1997; Blair, 1999; Hewitt, 1999; Bertran, 2003). Dating of deposits can aid in determining whether they were deposited in glacial or non-glacial times and hence help show whether glaciers could have been responsible for their formation. Using surface exposure dating with cosmogenic ^{10}Be, for example, Ballantyne and Stone (2004) used a Late Holocene age for a massive rock avalanche in Scotland to show that it was not associated with glacial ice, because glaciers did not exist in Scotland during the Holocene.

Tianchi Lake in Xinjiang is a well-known Chinese tourist site (Fig. 1). The origin of the lake has been highly debated and has intrigued researchers for many years. This is because the geomorphic and sedimentary characteristics of the landform that dams the lake indicate that it could have been produced by either glacial or mass movement processes. Many researchers have argued that Tianchi Lake formed during the latter part of the Last Glacial by glacial action that deepened the valley to produce a trough and then dammed it with a moraine (Han, 1981; Wang, 1981a; Wang, 1981b; Zheng and Ren, 1981; Zheng and Wang, 1983; Zheng, 1994). In contrast, some researchers believe that the ridge which dams the lake was the product of a landslide (Zhou and Zhao, 1962; Deng and Ding, 1989, 1990). To help resolve this debate, we re-examined the landform that blocks Tianchi Lake using geomorphological, sedimentological and geochronological techniques.

*Corresponding author. Tel./fax: +86 10 62849886.
E-mail address: clyi@itpcas.ac.cn (C. Yi).

1040-6182/$ - see front matter © 2006 Elsevier Ltd and INQUA. All rights reserved.
doi:10.1016/j.quaint.2006.02.011

2. Study area and sampling location

2.1. Field methods and sampling for cosmogenic radionuclide surface exposure dating

Tianchi Lake is located at 1920 m asl near Bogeda Peak, in the eastern Tianshan Mountain, and extends in a north-northeast direction with an area of 2.5 km^2 (Fig. 1). Bogeda Peak is composed of middle Carboniferous extrusive rock with grayish-green and grayish-dark tuff in the folded core, and wine-red andesitic volcanic breccia and grayish-green and dark-red tuff on both folded flanks that have been deformed into an anticline with the axis extending east to west. Tianchi Lake is located within the folded core that consists of grayish-green and wine-red tuff. In the vicinity of the lake, three sets of fractures with southwest, north-northeast and east-southeast directions form a network pattern. Interpretation from air photos (Han, 1981) shows that the trend of Tianchi Lake is controlled by tensional fractures that trend north-northwest.

A 1:50,000 scale topographic map was analyzed to determine the extent of the diamicton deposit that blocks Tianchi Lake. A sonar depth sounding device, model Piranha 4 (Humming Bird High Definition Sensor), was used to measure the approximate depth along the long axis of the lake. Sedimentary properties were examined in natural exposures and in excavations at construction sites. Two samples were collected on the highest tongue of the deposit for grain size analysis. Sample TCB was collected on the exposure next to the lake and DXTCB on the outer, downstream margin (Figs. 1 and 2).

Boulders which were collected for cosmogenic radionuclide (CRN) surface exposure dating are all dark-red andesite and grayish-green tuff. Samples for CRN dating

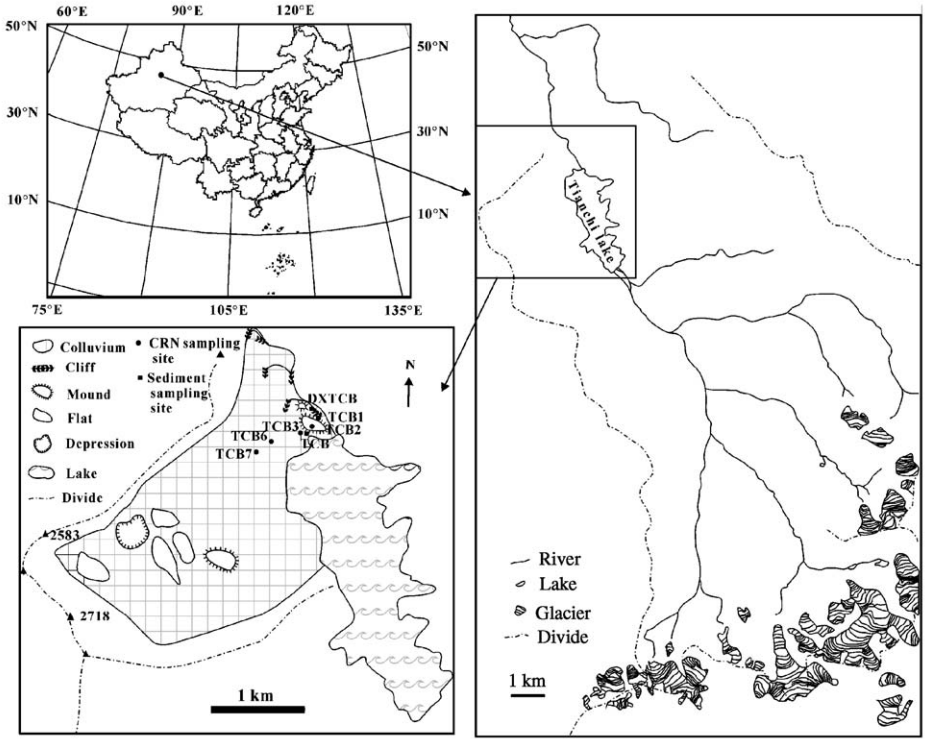

Fig. 1. Location of Tianchi Lake and the sampling sites.

Fig. 2. Sampling sites and views showing the characteristic sedimentary properties of the Tianchi diamicton deposit. (A) Coarse sediment on the diamicton deposit which is close to the source area of rock avalanche. (B) Fine sediment on the diamicton deposit which is farthest away from the source area of rock avalanche. Beyond is the scree from the upper sediment. (C) Part of fine sediment in Fig. 2B.

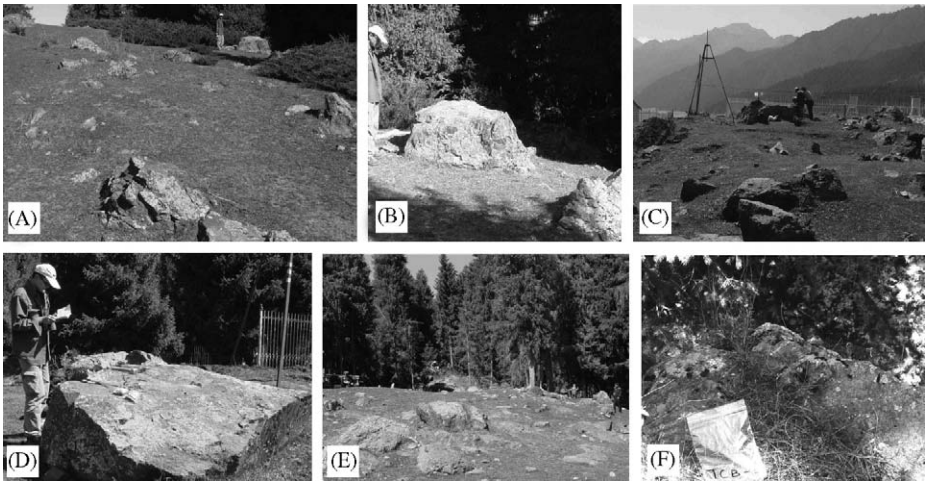

Fig. 3. Boulders within the Tianchi rock avalanche deposit. (A) Sampling site 1; (B) boulder sample TCB-1; (C) sampling site 3; (D) boulder sample TCB-3; (E) boulders on sampling site 6; (F) boulder sample TCB-6.

were collected by chiseling off a 1–2 cm thick layer of about 450 g of rock from the upper surfaces along the levee crests. Locations were chosen where there was no apparent evidence of exhumation or slope instability. Large boulders were chosen to help reduce the possibility that boulders may have been covered with snow for significant periods of the year (Figs. 1–3).

2.2. Laboratory methods

2.2.1. CRN dating

First, the samples were crushed and sieved. Quartz was then separated from the 250–500 μm size fraction using the method of Kohl and Nishiizumi (1992). After addition of a beryllium carrier, Be was separated and purified by ion exchange chromatography and precipitation at pH > 7. The hydroxides were oxidized by ignition in quartz crucibles. BeO was then mixed with Nb metal prior to determination of the $^{10}Be/^{9}Be$ ratios by accelerator mass spectrometry at the Center for Accelerator Mass Spectrometry in the Lawrence Livermore National Laboratory. The measured isotope ratios were converted to CRN concentrations in quartz using the total Be in the samples and the sample weights. Radionuclide concentrations were then converted to zero-erosion exposure ages using sea level high latitude (SLHL) ^{10}Be production rate of 5.16 at/g-quartz/yr (Stone, 2000). The Be production rate used is based on a number of independent measurements as discussed by Farber et al. (2005). Production rates were scaled to the latitude and elevation of the sampling sites using the star scaling factors of Lal and Peters (1967) and Lal (1991) and an assumed 3% SLHL muon contribution, and were further corrected for changes in the geomagnetic field over time. However, there is considerable debate regarding the technique and magnitude of this correction (Nishiizumi et al., 1996; Masarik and Wieler, 2003; Pigati and Lifton, 2004). We, therefore, present geomagnetically corrected ages in Table 1, but in the discussion that follows we use the ages that are not corrected for fluctuations in the paleomagnetic field. Details of the calculation are given in Farber et al. (2005).

2.3. Grain size analysis

The organic matter and calcite in the samples were removed by hydrogen peroxide and sparse hydrochloric acid, respectively. Using 1 g (dried weight) of each organic- and carbonate free sample in 2 ml of Calgon (1 l Calgon contains 33 g of $(NaPO_3)_6$ and 7 g of Na_2CO_3) with 20 ml of distilled water, the suspended sediment was dispersed using an ultrasonic device. About 4 ml of the suspension was analyzed by the laser grain size analyzer MASTERSIZER 2000, with size limits of 0.02–2000 μm.

3. Results

3.1. Geomorphology

The Tianchi diamict is 1300 m long from north to south and 700 m wide at the outlet of the lake. The landform consists of three tongues that overlap each other at different elevations, and form two boulder hills on the highest tongue (Fig. 1).

The eastern hillside toward Tianchi Lake is steep, with a slope of 27–30°, while the western hillside is gentle with a slope of ~11°. Several rock platforms, 200–350 m long and 350–450 m wide, with huge blocks of rock concentrated on the top at an elevation of 2200–2350 m, are present on the western slope. A depression, locally called the "Pan-shaped Pit", has an area of 350 × 350 m^2 at an elevation of 2200 m (Figs. 1 and 4). A small, 20–50 m high ridge is present at its front, dipping back toward the cliff. The depression has an undulating surface covered with blocks of rock and thus was previously understood to be a glacial cirque

Table 1
Cosmogenic radionuclide surface exposure dating data and results

Sample name	Latitude/Longitude	Altitude (m)	Boulder dimensions (length, width and height, cm)	Lat/alt correction	Depth/ topography correction	Be-10 concentration (atoms/g of quartz $\times 10^3$)	Be-10 age (years)
TCB-1	43°54.122′/88°07.321′	1923	158/127/70	4.56	0.98	252±25	11,008±1036[a] 10,911±1027[b]
TCB-2	43°54.049′/88°07.271′	1944	516/340/124	4.63	0.98	410±14	17,662±5819[a] 17,322±5706[b]
TCB-3	43°53.984′/88°07.266′	1938	242/165/74	4.61	0.98	302±40	13,131±1735[a] 13,003±1718[b]
TCB-6	43°53.806′/88°07.077′	1944	730/463/322	4.63	0.98	253±14	10,879±595[a] 10,784±590[b]
TCB-7	43°53.877′88°07.159′	1922	617/304/105	4.56	0.98	166±15	7259±6608[a] 7268±6616[b]

[a]Not corrected for paleomagnetic variations.
[b]Corrected for paleomagnetic variations using data from Ohno and Hamamo (1992), McElhinny and Senanayake (1982) and the SINT-800 record (Guyodo and Valet, 1999).

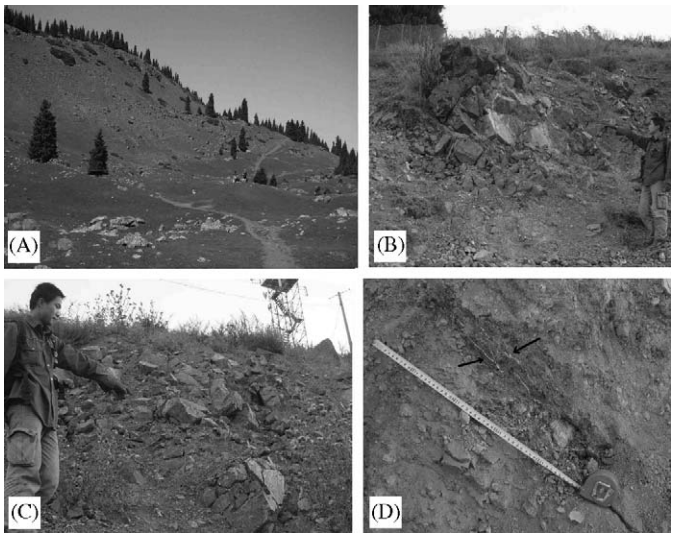

Fig. 4. (A) Depression in upper western slope. Counter slope of landslide in the upper hillside; (B) and (C) crackled rock in the exposure; (D) crackled rock and veins. The arrow shows that the quartz veins extend parallel to each other.

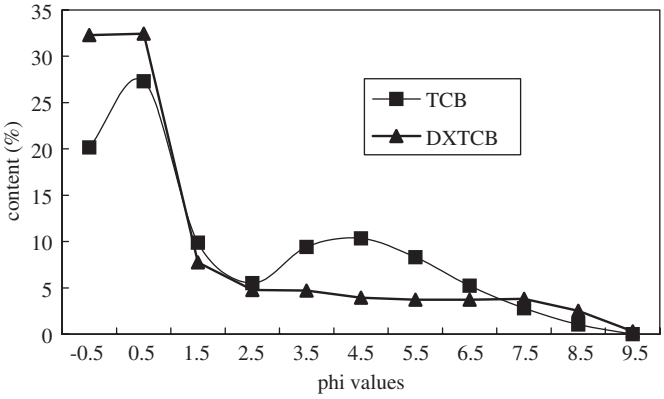

Fig. 5. Particle size distributions of rock avalanche in fine fraction.

(Han, 1981). Zheng (1994) described the western slope, and said that it was composed of a fan-shaped loose deposit of debris with a slope of 12° and an area of $2.5 \times 1.8\,km^2$, confined laterally by cliffs on other three sides.

Sonar showed that the bottom of the lake is uneven and slopes gently from the delta to a depth of 60–70 m where the bottom flattens out. At about three-fifths of the whole distance from the delta, the bottom becomes uneven with a greatest depth of 150 m.

3.2. Sedimentology

The sediments within the landform comprise diamicton with monomictic angular clasts. Large numbers of cracked boulders, 1–2 m in diameter, are present within the exposures along the track next to the lake. These clasts have been crushed into 10–30 cm size pieces, and although the pieces are separated, the outline of the original boulder's shape can be seen. The cracked clasts are angular, fitting together like pieces of a jig-saw puzzle to form 'ghost rocks'. Some boulders have been crushed into pebbles, sand and silt-sized particles (Fig. 5, Sample TCB). The quartz veins in the boulders were also comminuted, but they still remain in the profile without apparent displacement (Fig. 4D). These crushed sandy grains and small pebbles are also angular. There is a large exposure at the cliff on the margin of the highest tongue (Fig. 1). The sediment is 70 m thick and its surface is armored with boulders. Some of this has failed and forms a talus slope near the foot of the exposure (Fig. 2B). The other part of the exposure comprises red and grayish-white crushed clasts, most of which are 2–5 cm in diameter with a few angular clasts up to 10–20 cm in diameter (Figs. 2B and C).

3.3. Particle size

The coarse sand fraction (0.5–1 mm, 0.5–0 ∅) is the dominant particle size in Sample TCB, but fine sand and silt with grain sizes of 0.125–0.032 mm (3–6 ∅) are also common. In comparison, the 0.5–2 mm (0.5 to −1 ∅) particle size is most common in Sample DXTCB with abundant silt fractions (Fig. 5).

3.4. Cosmogenic radionuclide surface exposure dating

We attempted to date seven boulder samples. However, two of the samples did not yield any quartz. The results for the remaining five samples are shown in Table 1. The quartz yields of samples TB2 and TB7 were small (~5 g each) and the large errors associated with these are a result of low AMS counting values. Fig. 6 plots the ages and shows the probability distribution for the data. These probability distributions suggest that the ages cluster at around 12 ka.

4. Discussion

Our study of the geomorphological features suggests that the diamicton originated through excavation of the adjacent valley slopes by rock avalanching. A pan-shaped depression on the upper landslide was believed previously to have been an early Pleistocene glacial cirque (Wang, 1981a, b; Yan and Wang, 1981). However, the geomorphological features of the several small platforms interlacing at the upper slumping end (Fig. 1) suggest that they are stair stepping platforms produced along the slipping planes in a large landslide and Pan-shaped Pit is a small depression formed by the counter-dipping slope in the platform.

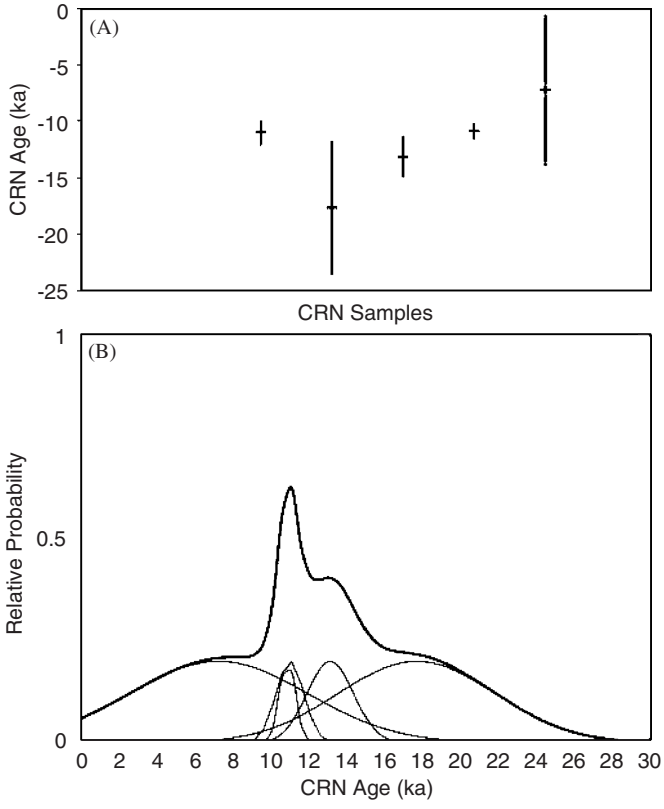

Fig. 6. CRN ^{10}Be surface exposure dates for the levee. (A) The mean value that is shown refers to the mean of the data and the error bar is expressed as an absolute value; (B) probability plots of the CRN data.

It is particularly notable that the deposit can be traced from the slope into the lake, where it comprises of an irregular arrangement of hummocks. Based on an underwater relief map that was produced by Yuan (unpublished map of Tianchi, 1930), drafted using sounding wire, Zheng (1994) drew profiles along and across the lake which show two deep depressions and a bulge between them with a relative height of 20–40 m. He ascribed their origins as glacial-eroded depression and glacial-eroded rock step, respectively. Based on the air photos, Han (1981) interpreted the Tianchi levee as a fan-shaped landslip body present under water on the western bank of the lake. Using the soundings of Yuan (unpublished map of Tianchi, 1930), we found that the bottom is of low relief for the upstream three-fifths of the lake. The part of the lake near the levee undulates on a much larger scale. This part of the underwater landform is similar to the southeastern part of the landslide, thus becoming an integrated landslide body (Fig. 1).

The sedimentary characteristics of this deposit are also similar to those described for rock avalanches from other high mountain regions (Johnson, 1978; Owen, 1991, 1993; Bishop, 1997; Friedmann, 1997; Blair, 1999; Hewitt, 1999; Barnard et al., 2001; Bertran, 2003; Ballantyne and Stone, 2004). In particular, the ghost rocks and crackled texture are very common characteristics of rock avalanche deposits (Johnson, 1978). The reverse grading and boulder armoring is indicative of mass movement mechanisms (cf. Owen, 1991, 1993).

Prior to these dating results, the age of the formation was thought to be any time during the late or early Pleistocene (Yan and Wang, 1981). However, the cosmogenic dating shows that the landform formed during the Lateglacial, most likely during the Younger Dryas Stade. There is little evidence in Tibet or the bordering mountains for a Younger Dryas glacial advance (see Owen et al., 2005) and therefore these ages help support the sedimentological evidence that this is a landslide deposit rather than a moraine because there were no glaciers in the valley at this time to produce such a landform.

5. Conclusions

The geomorphological, sedimentological and geochronological critera indicate that the diamict deposit that help form Tianchi Lake were deposited during the Lateglacial, and possibly during the Younger Dryas Stade, by rock avalanching processes. The results highlight the usefulness of using multidisciplinary approaches to help determine the origin of problematic landforms to aid in understanding

the landscape evolution and/or paleoenvironmental history of high mountain regions.

Acknowledgments

This work was supported by Chinese Academy of Sciences Grant ZKY-2004-3, NSFC Grant 40271016, the LICCRE Grant BX2001-02, the 100 Talents project of the CAS, 2005, and Tianshan Glacier Observatory, University Campus Laboratory Collaboration Program of the University of California. This work was performed under the auspices of the US Department of Energy by the University of California, Lawrence Livermore National Laboratory, under Contract No. W-7405-Eng-48.

References

Ballantyne, C.K., Stone, J.O., 2004. The Beinn Alligin rock avalanche, NW Scotland: cosmogenic ^{10}Be dating, interpretation and significance. Holocene 14 (3), 448–453.

Barnard, P.L., Owen, L.A., Sharma, M.C., Finkel, R.C., 2001. Natural and human-induced landsliding in the Garwhal Himalaya of Northern India. Geomorphology 40, 21–35.

Bertran, P., 2003. The rock-avalanche of February 1995 at Claix (French Alps). Geomorphology 54 (3–4), 339–346.

Bishop, K.M., 1997. Miocene rock-avalanche deposits, Halloran/Silurian Hills area, southeastern California. Environmental & Engineering Geoscience 3 (4), 501–512.

Blair, T.C., 1999. Form, facies, and depositional history of the North Long John rock avalanche, Owens valley, California. Canadian Journal of Earth Sciences 36 (6), 855–870.

Deng, X.F., Ding, Y.J., 1989. Discussion on the Ice Age of Tianchi. Annals of Tianshan Glacier Observatory in 1988 (Chinese with English summary) No. 7.

Deng, X.F., Ding, Y.J., 1990. Landslide Dam and Tianchi Lake near Urumqi, Xinjiang, China. Landslide News No. 4 (July, 1990), pp. 23–25.

Farber, D.L., Hancock, G.S., Finkel, R.C., Rodbell, D., 2005. The age and extent of tropical glaciation in the Cordillera Blanca, Peru. Journal of Quaternary Science 20, 759–776.

Friedmann, S.J., 1997. Rock-avalanche elements of the Shadow Valley basin, eastern Mojave desert, California: processes and problems. Journal of Sedimentary Research 67 (5), 792–804 (Part A).

Guyodo, Y., Valet, J.-P., 1999. Global changes in intensity of the Earth's magnetic field during the past 800 kyr. Nature 399, 249–252.

Han, S.D., 1981. Primary cognition on Tianchi Lake. In: Geology Association of China and Geology Association of Xinjiang (Eds.), Selected Papers on Quaternary Geology and Glaciations in Xinjiang. Xinjiang People Press, Urumqi, pp. 143–147.

Hewitt, K., 1999. Quaternary moraines vs catastrophic rock avalanches in the Karakoram Himalaya, northern Pakistan. Quaternary Research 51 (3), 220–237.

Johnson, B., 1978. Blackhawk landslide, California, USA. In: Voight, B. (Ed.), Rockslides and Avalanches. Elsevier Scientific Publishing Company, New York, pp. 481–504.

Kohl, C.P., Nishiizumi, K., 1992. Chemical isolation of quartz for measurement of in situ-produced cosmogenic nuclides. Geochimica et Cosmochimica Acta 56, 3583–3587.

Lal, D., 1991. Cosmic ray labeling of erosion surfaces: In situ nuclide production rates and erosion models. Earth and Planetary Science Letters 104, 429–439.

Lal, D., Peters, B., 1967. Cosmic ray produced radioactivity on the Earth. In: Sitte, K. (Ed.), Handbuch der Physik, vol. 4612. North-Holland, Amsterdam, pp. 551–612.

Masarik, J., Wieler, R., 2003. Production rates of cosmogenic nuclides in boulders. Earth and Planetary Science Letters 216, 201–208.

McElhinny, M.W., Senanayake, W.E., 1982. Variations in the geomagnetic dipole 1: the past 50,000 years. Journal of Geomagetism and Geoelectricity 34, 39–51.

Nishiizumi, K., Finkel, R.C., Klein, J., Kohl, C.P., 1996. Cosmogenic production of ^{7}Be and ^{10}Be in water targets. Journal of Geophysical Research 101, 22225–22232.

Ohno, M., Hamamo, Y., 1992. Geomagentic poles over the last 10,000 years. Geophysical Research Letters 19 (16), 1715–1718.

Owen, L.A., 1991. Mass movement deposits in the Karakoram Mountains: their sedimentary characteristics, recognition and role in Karakoram landform evolution. Zeitschrift für Geomorphologie 35 (4), 401–424.

Owen, L.A., 1993. Glacial and non-glacial diamictons in the Karakoram Mountains. In: Croots, D., Warren, W. (Eds.), The Formation and Deformation of Glacial Deposits. A.A. Balkema, Rotterdam, pp. 9–29.

Owen, L.A., Finkel, R.C., Barnard, L.P., Ma, H., Ashai, K., Caffee, M.W., Derbyshire, E., 2005. Climatic and topographic controls on the style and timing of Late Quaternary glaciation throughout Tibet and the Himalaya. Quaternary Science Reviews 24 (12–13), 1391–1411.

Pigati, J.S., Lifton, N.A., 2004. Geomagnetic effects on time-integrated cosmogenic nuclide production with emphasis on in situ C-14 and Be-10. Earth and Planetary Science Letters 226, 193–205.

Stone, J.O., 2000. Air pressure and cosmogenic isotope production. Journal of Geophysical Research 105, 23,753–23,759.

Wang, S.J., 1981a. Division of Quaternary Glaciation and Ice Age in North and South of Bogeda, North Tianshan. In: Geology Association of China and Geology Association of Xinjiang (Eds.), Selected Papers on Quaternary Geology and Glaciations in Xinjiang. Xinjiang People Press, Urumqi, pp. 107–114.

Wang, Z.C., 1981b. Ancient Process Glacial of Tianshan. In: Geology Association of China and Geology Association of Xinjiang (Eds.), Selected Papers on Quaternary Geology and Glaciations in Xinjiang. Xinjiang People Press, Urumqi, pp. 91–106.

Yan, J.H., Wang, C.L., 1981. Division of Quaternary Glaciation and Stratum in North Bogeda, East Tianshan, Xinjiang. In: Geology Association of China and Geology Association of Xinjiang (Eds.), Selected Papers on Quaternary Geology and Glaciations in Xinjiang. Xinjiang People Press, Urumqi, pp. 115–126.

Zheng, B.X., 1994. Discussion on the formation of Tianchi Lake in Xinjiang. Arid Land and Geography (Chinese with English summary) 17 (1), 68–75.

Zheng, B.X., Ren, B.H., 1981. Evolvement history of Quaternary Glacial in North Slope Bogeda, Tianshan. In: Geology Association of China and Geology Association of Xinjiang (Eds.), Selected Papers on Quaternary Geology and Glaciations in Xinjiang. Xinjiang People Press, Urumqi, pp. 194–195.

Zheng, B.X., Wang, C.N., 1983. Discussion on the Quaternary Glacier of Bogeda Area, Tianshan. Journal of Glaciology and Geocryology (Chinese with English summary) 5 (3), 123–132.

Zhou, T.R., Zhao, J., 1962. Geomorphological Conditions for Development of Agriculture and Pasture Husbandry in Xinjiang. Geography (Chinese with English summary), pp. 46–51.